Search for Microscopic Black Holes in Multijet Final States with the ATLAS Detector using 8 TeV *pp* Collisions at the LHC[1]

Asif Siddique

ICTP-NCP School on LHC Physics

November 19, 2014

[1] PhD Thesis @ University of Alberta, Canada

Motivation

Hierarchy Problem

Why is there a large difference between the Electroweak scale (M_{EW} ~0.1 TeV) and the Planck scale (M_P ~10^{16} TeV)

or

Why gravity appears weaker as compared to the SM forces ?

Low-scale gravity models propose a solution to this problem with the concept of extra spatial dimensions by observing microscopic black holes in high energy particle collisions.

Black Holes

Astronomical Black Holes

A spacetime region with sufficiently compact mass produces an immense gravitational pull to prevent everything including light, from escaping. Classically, an event horizon is a surface around the a Black Hole which is called **point of no return**. Anything that touches event horizon, will be trapped and won't go back.

Microscopic Black Holes

In high energy particle collider, mini Black Holes can be produced if there is a strong gravity at small scales. Microscopic Black Holes will evaporate **quickly** unlike astronomical Black Holes.

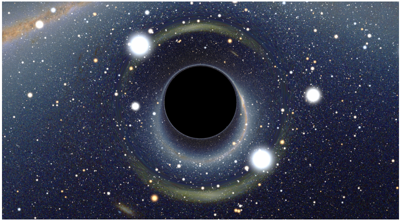

Fundamental Particles

- There are two type of particles in nature **fermions** and **bosons**.
- In fermions, **Quarks** and **Leptons** are the fundamental particles only.
  - Generally quarks exist in bound states, called Hadrons.

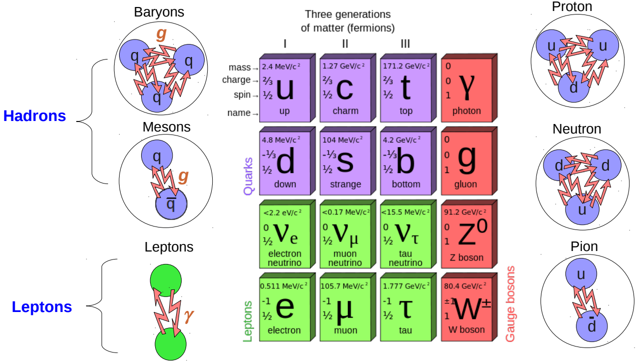

- How do they interact?

Fundamental Forces

- All the particles interact via **four fundamental forces** in nature
- Standard Model of particle physics incorporates Electromagnetic, Weak and Strong forces but doesn't include gravity.

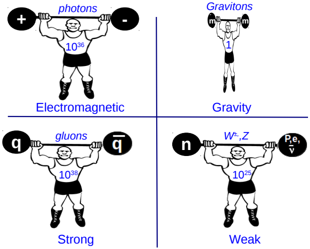

- Gravity appears to be much weaker than other forces.
- Is gravity really a very weak force?

Extra-dimensions and Strong Gravity

- Gravity is the only force that can propagate in **extra dimensions** and most of its strength is spent in extra dimensions.
- At current fundamental scale 10^{-18} m we are not able to see extra-dimensions that's why gravity appears to be very weak.

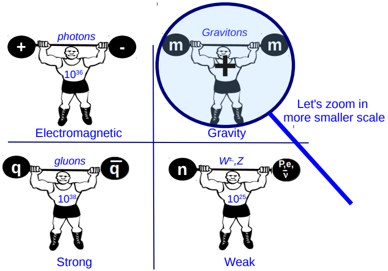

- If we go beyond the fundamental scale then we may see **extra dimensioned** and **strong gravity at low scale**

Low-scale Gravity

- **In ADD model**, there are large extra dimensions and only gravity can propagate in extra spatial dimensions (n).
- The extra dimensions are compactified in a sphere of radius $\mathscr{R}$, e.g., $\mathscr{R} \sim$ submillimeter scale for $n \geq 3$.
- At such a low scale ($\sim \mathscr{R}$), gravity will appear as strong as other forces, i.e., the apparent Plank scale (M_P) reduces to the true Planck scale (M_D[2]).
- As a consequence of strong gravity at low-scale, **production of microscopic black holes** (MBH) is possible in a high energy collision under certain conditions.

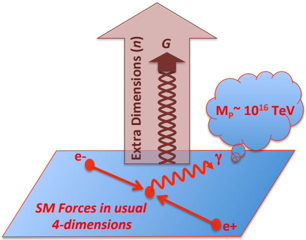

ADD Model of large extra dimensions

Extra dimensions (*n*) are compactified in a sphere

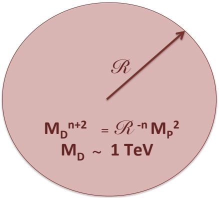

[2] where $D = n + 4$, total number of dimension

MBH Formation and Decay

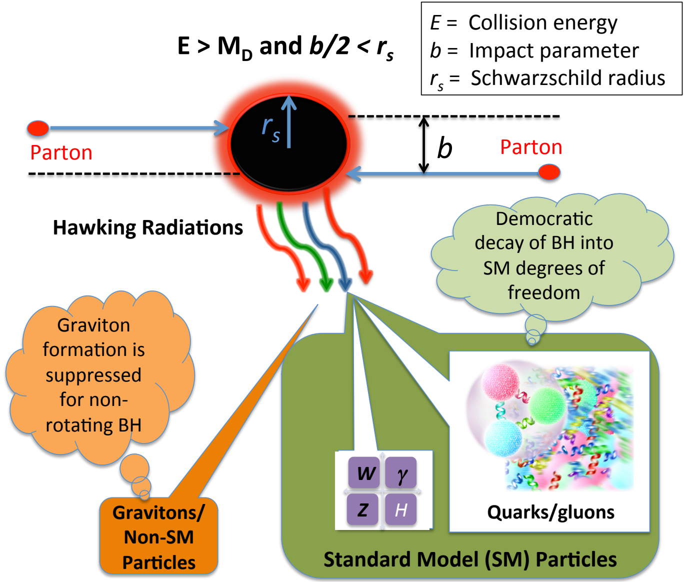

MBH Signals in Multjet Final States

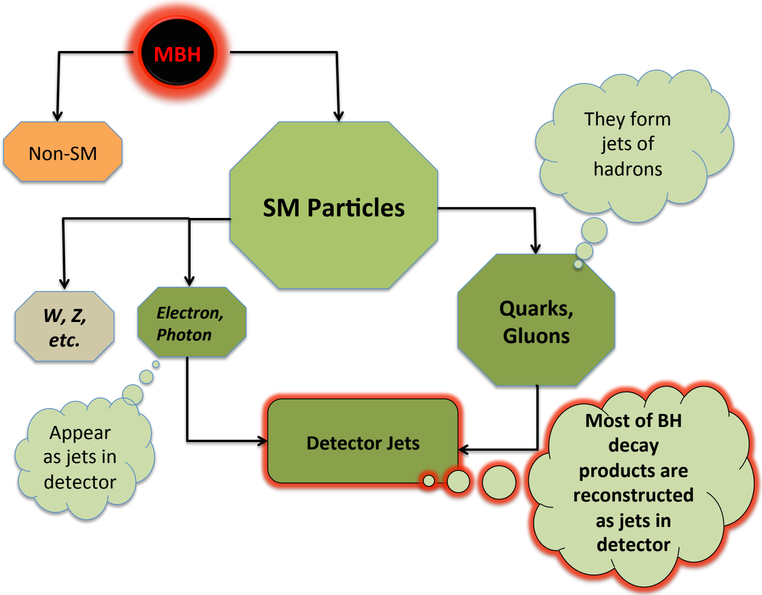

Microscopic Black Holes at the LHC

- MBH may be produced in high energy proton-proton (pp) collisions at the Large Hadron Collider (LHC).
- Once produced, MBH may be distinguished by
  - high jet multiplicity (N),
  - democratic (with equal probabilities) and
  - highly isotropic (same in all directions) decays

  with the final state particles carrying **hundreds of GeV of energy**.
- Hence,
  - high-N, and
  - high-p_T (transverse momentum)

  are the key signatures of MBH.

Therefore, we select ***multijet final states with high sum of p_T*** *in the data recorded by the ATLAS detector at the LHC.*

ATLAS Detector at the LHC

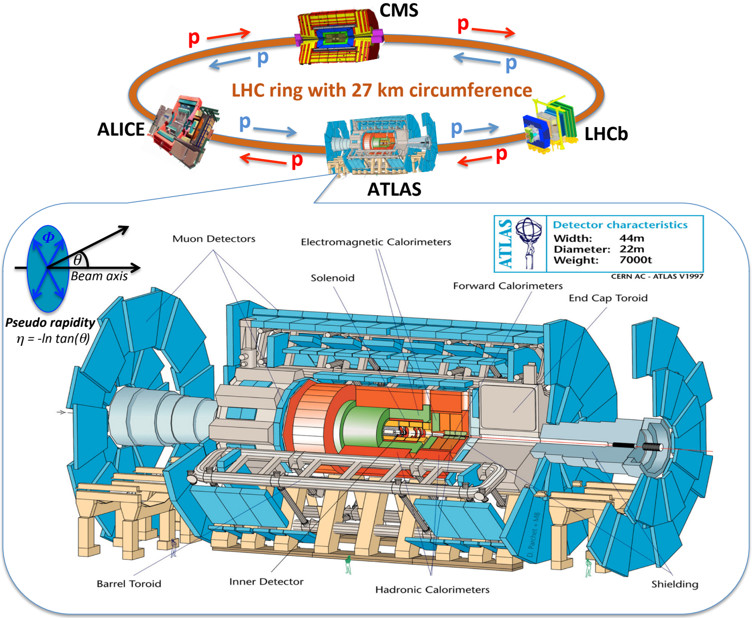

Datasets

ATLAS 2012 data

- *pp*-collisions with 8 TeV centre of mass energy.
- An integrated luminosity of 20.34 fb^{-1}.

Dijet Monte Carlo Simulations (MCs)

Two types of MCs are used in this study.

- PYTHIA dijet
- HERWIG++ dijet

In this study, events with **high sum p_T** *are studied for different* **jet multiplicities** *for both the data and MCs.*

The Main Kinematic Variable, H_T

- The main kinematic variable chosen is H_T, which is the scalar sum of jet p_T, i.e., $H_T = \sum p_T$ if $p_T > 50$ GeV and $|\eta| < 2.8$

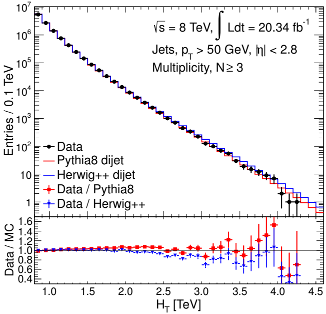

- For different jet multiplicities, H_T distributions are expected to be **shape invariant**[3] because of the collinear nature of the initial and final state radiation, which does not change the total transverse kinematics of the system.

- H_T **shape invariance** is investigated by observing the ratio of the inclusive jet multiplicities $N \geq 3, 4, ..., 7$ with respect to dijet multiplicity $N = 2$ (chosen as the baseline case).

[3] above a certain kinematical threshold

Dijet Multiplicity: A Baseline for Background Estimation

Dijet case is used as the baseline case to define **the control region** because

- MBH are expected to produce high jet multiplicities, therefore, the lowest multiplicity $N = 2$ case is chosen as the baseline case for the QCD background[4] estimation.
- Dijet case is **well-studied** in the ATLAS and CMS collaborations, and no evidence of any resonance or new physics have been found.

Hence, the shape of the dijet-H_T is used to estimate background for the higher jet multiplicities $N \geq 3, 4, .., 7$, on the basis of shape invariance assumption.

[4] Main background in this study

H_T Shape Invariance

- The H_T ratios of inclusive jet multiplicities $N \geq 3, 4, .., 7$ with respect to $N = 2$ are examined for the shape invariance above a certain kinematical threshold. An example of the H_T ratio ($H^{\text{inl}}_{T_{52}} \equiv$ Ratio of inclusive multiplicity $N \geq 5$ to $N = 2$), is shown in figure.

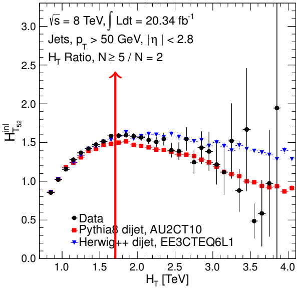

- A lower threshold for shape invariance, $H_T > 1.7$ TeV, is chosen for all the jet multiplicities.

- Different upper thresholds are studied to get a region with best shape invariance, which is defined as the normalization region.

At this stage, we can define three kinematical regions in the study.

The Three Kinematical Regions

- The control region (CR):
  $H_T > 1.7$ TeV and $N = 2$
  - the region where no new physics is expected.

- The normalization region (NR):
  $1.7 < H_T < 2.4$ TeV and $N > 2$
  - the region of best shape invariance
  - non-black hole region

- The signal region (SR):
  $H_T > 2.4$ TeV and $N > 2$
  - the region beyond the NR

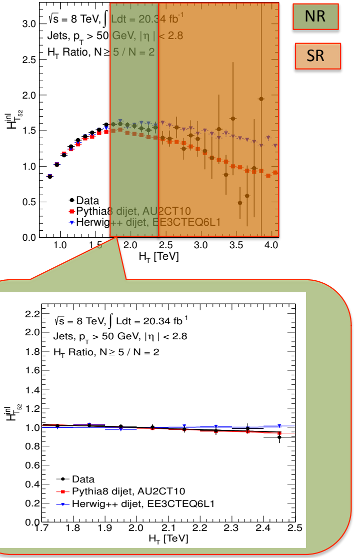

Now we can go towards background estimation.

The main QCD background is determined from the data.

- The H_T distribution for the dijet (CR) is fitted by an ansatz function
$$f(x) = \frac{p_0(1-x)^{p_1}}{x^{p_2+p_3 \ln x}},$$
where $x = H_T/\sqrt{s}$ and $\sqrt{s} = 8$ TeV. p_0, p_1, p_2 and p_3 are the fit parameters.

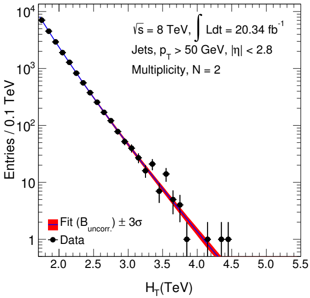

- The shape of dijet function normalized by a factor[5], is applied to $N > 2$ to estimate the background in the SR.
$$[f(x)]^{N>2} = n_f \times [f(x)]^{N=2}$$

- The background estimation relies on the H_T shape invariance.

We need to investigate the H_T shape invariance carefully.

[5] Normalization factor $n_f = H_T^{N>2}/H_T^{N=2}$ is a number, obtained from the NR

In the NR (Data and MCs)

- A linear-fit is applied to the H_T ratios, e.g. $H^{\text{inl}}_{T_{52}}$ for the data and MCs.
- For perfect shape invariance, the linear fit should have slope consistent with zero.
- The shape invariance is not perfect and definitely there are some **effects due to non-invariance**.

Example of Linear Fit in the NR

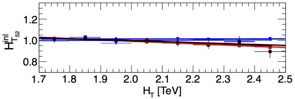

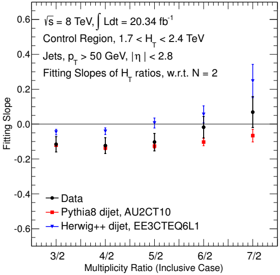

In the SR (MCs)

- By the same method, the H_T ratios for the MCs also indicate some **effects due to non-invariance**.

The non-invariant effects cause **an overestimation of the background** *in the SR, therefore, the data-driven background is corrected based on the correction factors derived from MCs.*

Corrections to the Background Estimation

- For jet multiplicities $N > 2$, the nominal background (data-driven) without any correction is denoted as

$$\mathrm{B_{uncorr}} \equiv [f(x)]^{N>2}$$

- The effects due to non-invariance in the SR of the H_T distribution are compensated by applying a $\mathrm{CF^{MC}}$ (correction factor derived from the MCs) extracted from the invariance trend of both the MCs, i.e.,

$$\mathrm{B_{corr}} = \mathrm{CF^{MC}} \times \mathrm{B_{uncorr}}$$

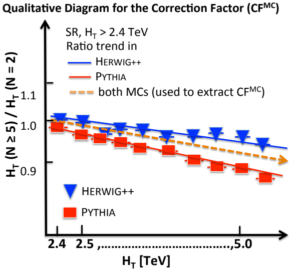

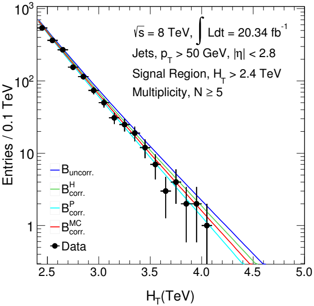

Summary of Background Estimation

Following are the steps:

- Function fitting to the CR ($N = 2$)
  - An ansatz function is fitted to the dijet case, i.e., $[f(x)]^{N=2}$.
- Normalizing CR-fit to the higher multiplicities ($N > 2$)
  - On the basis of shape invariance
    $$[f(x)]^{N>2} = n_f \times [f(x)]^{N=2} \equiv \mathrm{B_{uncorr}}$$
- Applying correction factors to the background estimation
  - On the basis of MCs
    $$\mathrm{B_{corr}} = \mathrm{CF^{MC}} \times \mathrm{B_{uncorr}}$$

What are the uncertainties involved in the background estimation ?

Systematic Uncertainties

There are three types of systematic uncertainties on the background estimation involved in this study.

- Corrections to non-invariance (ΔB_{corr})
  - The CF^{MC} derived from straight line fit over the H_T ratio in the SR, introduces largest uncertainty in the study.
  - Computed from the errors and differences of fit parameters of two MCs.
- Jet Energy Uncertainties (ΔB_{jeu})
  - Jet Energy Scale (JES) and Jet Energy Resolution (JER) uncertainties.
  - Estimated by comparing distributions with and without JES/JER.
- Choice of the NR (ΔB_{nf})
  - The NR, $1.7 < H_T < 2.4$ TeV, is slided ± 0.1 TeV on the boundaries to quantify its effects on the background estimation.

The amount of total uncertainty remains within 15-70% range in the $2.4 < H_T < 4.5$ TeV of the SR, depending upon the (N, H_T).

Data, Background and Signal

CHARYBDIS2 BH simulations are being used in these plots

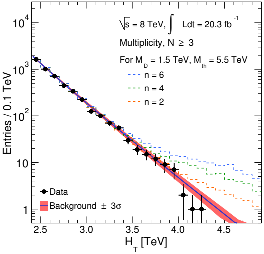

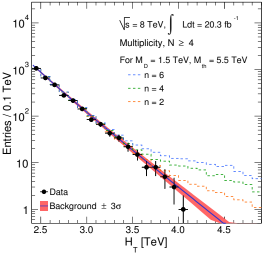

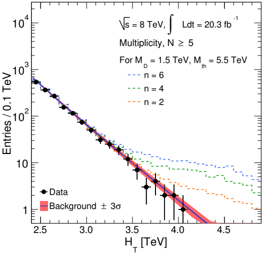

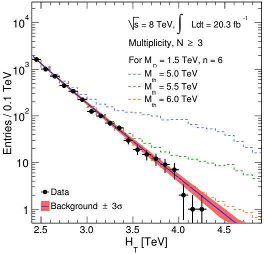

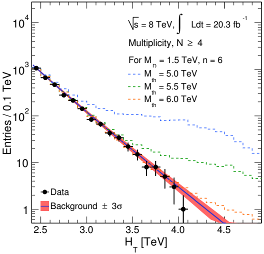

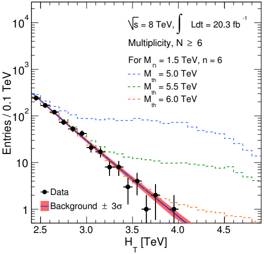

Data Vs Background in the SR

- In the SR ($H_T > 2.4$ TeV), let's define another variable H_T^{min}, i.e.,

$$H_T > H_T^{\mathrm{min}}$$

which means we consider SR with different lower thresholds, e.g., 2.4 TeV and above, 2.5 TeV and above, etc.

- The comparison of the data and estimated background along with the band of total uncertainty, as a function of H_T^{min} is shown for $N \geq 6$ and $N \geq 7$ (as examples).

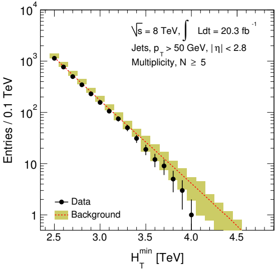

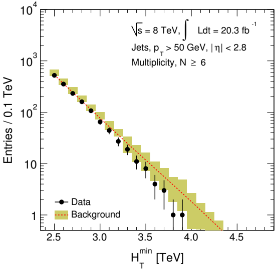

Typically, the data are in one sigma agreement to the background.

Data Vs Background in H_T^{min}

H_T^{min} (TeV)	Multiplicity $N \geq 3$		Multiplicity $N \geq 4$		Multiplicity $N \geq 5$		Multiplicity $N \geq 6$		Multiplicity $N \geq 7$	
	N^{data}	N^{bkg}	N^{data}	N^{bkg}	N^{data}	N^{bkg}	N^{data}	N^{bkg}	N^{data}	N^{bkg}
3.5	66	$78.6^{+13.8}_{-8.2}$	40	$49.9^{+10.7}_{-6.6}$	19	$26.3^{+8.3}_{-9.3}$	8	$11.7^{+4.5}_{-4.5}$	2	$4.5^{+2.6}_{-2.1}$
3.6	47	$54.6^{+9.4}_{-6.9}$	25	$34.5^{+7.5}_{-4.8}$	12	$18.2^{+5.7}_{-6.8}$	4	$8.1^{+2.9}_{-3.5}$	2	$3.1^{+1.3}_{-1.7}$
3.7	32	$37.9^{+6.8}_{-9.4}$	17	$23.9^{+6.3}_{-9.2}$	9	$12.6^{+4.3}_{-5.1}$	3	$5.6^{+2.6}_{-2.5}$	2	$2.1^{+0.9}_{-1.2}$
3.8	20	$26.3^{+5.3}_{-11.0}$	9	$16.6^{+4.2}_{-7.1}$	5	$8.7^{+2.8}_{-3.8}$	1	$3.8^{+1.6}_{-2.1}$	1	$1.4^{+0.6}_{-0.9}$
3.9	11	$18.3^{+3.8}_{-8.4}$	4	$11.5^{+4.5}_{-5.2}$	3	$6.0^{+2.2}_{-2.8}$	1	$2.6^{+2.3}_{-1.4}$	1	$1.0^{+0.5}_{-0.9}$
4.0	4	$12.7^{+3.1}_{-6.3}$	1	$7.9^{+5.0}_{-3.9}$	1	$4.1^{+1.4}_{-2.2}$	0	$1.8^{+0.8}_{-1.3}$	0	$0.7^{+0.3}_{-0.6}$
4.1	2	$8.7^{+4.0}_{-4.9}$	0	$5.5^{+8.0}_{-2.9}$	0	$2.8^{+1.7}_{-1.8}$	0	$1.2^{+0.4}_{-0.7}$	0	$0.5^{+0.2}_{-0.3}$
4.2	1	$6.0^{+1.5}_{-4.6}$	0	$3.7^{+0.9}_{-2.2}$	0	$1.9^{+0.6}_{-1.2}$	0	$0.8^{+0.3}_{-0.5}$	0	$0.3^{+0.1}_{-0.2}$

Counting Experiment for Limits

- In order to calculate model-independent limits, number of events for the data, background and systematic uncertainties are computed as a function of H_T^{min} in the SR.
- For example, for $N \geq 5$, all the numbers in terms of number of events are given with their corresponding H_T^{min} are:

H_T^{min} (TeV)	Data	B_{corr}	ΔB_{corr}	ΔB_{jeu}	ΔB_{nf}
2.4	1675	1759.10	382.43	17.77	23.40
2.5	1134	1181.35	257.77	16.65	15.71
2.6	770	797.07	175.04	8.21	10.60
↓	↓	↓	↓	↓	↓
↓	↓	↓	↓	↓	↓
↓	↓	↓	↓	↓	↓
4.0	1	4.37	1.26	2.94	0.06
4.1	0	3.04	0.90	1.52	0.04

Model-Independent Limits

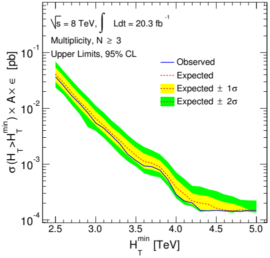

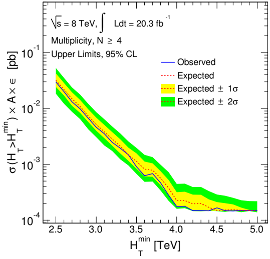

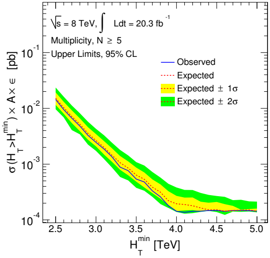

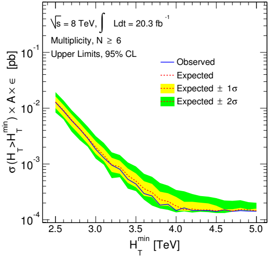

$\sigma \times A \times \epsilon$ is
0.29 fb to 1.14 fb
for
$N \geq 3$ to $N \geq 7$
for
$H_T > 4.0$ TeV

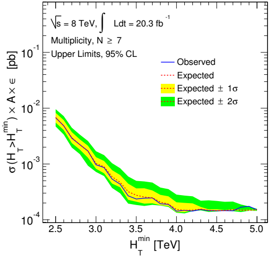

Upper limits on the cross-section times acceptance times efficiency ($\sigma \times A \times \epsilon$) with 95% confidence level (CL), on the production of new physics.

Model-Dependent Limits

- CHARYBDIS2 BH simulations are used for non-rotating black holes.
- Different black hole samples as a function of extra dimensions n, minimum mass to produce BH M_{th} and true Planck scale M_D are used to compute the exclusion limits.
- The crossing points of theoretical cross sections and upper limits are used to convert upper limits to lower limits.

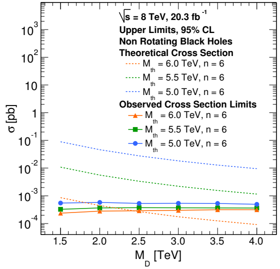

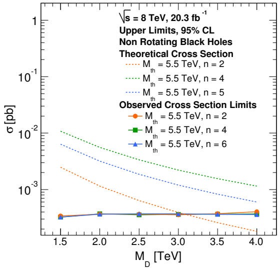

Exclusion Limits ATLAS Vs. CMS

Model-Independent Upper Limits

Model-independent upper Limit on $\sigma \times A \times \epsilon$ (fb)		
CMS (for 3.7 fb^{-1})	CMS (for 12.1 fb^{-1})	ATLAS (for 20.3 fb^{-1})
0.70	0.20	0.15

Model-Dependent Lower Limits

n	M_D (TeV)	Model-dependent lower limits on M_{th} (TeV)		
		CMS (for 3.7 fb^{-1})	CMS (for 12.1 fb^{-1})	ATLAS (for 20.3 fb^{-1})
2	3.5	4.9	5.2	5.4
4	3.0	5.4	5.6	5.8
6	2.5	5.7	5.9	6.0

Our results have improved exclusion limits.

Conclusions

- QCD Background
  - Dijet multiplicity is the CR to estimate the background for $N > 2$.
  - QCD background is determined from the data on the basis of H_T shape invariance for different jet multiplicities.
  - The correction factors due to non-invariance are derived from MCs, and applied to the data-driven background estimation.

- The Data are in agreement to the background within one sigma.
  - No new physics have been found in the ATLAS 2012 data.
  - Exclusion limits are set on the production of new physics.

- Model-Independent and model-dependent exclusion Limits are set at the 95% CL.

Thanks

Backup slides

Chi-Squared ($\chi^2 = \sum \frac{(Obs-Exp)^2}{Exp}$) Test

- The calculated chi square value can be used to obtain probabilities, or P values, from a chi square table
  - These probabilities allow us to determine the likelihood that the observed deviations are due to random chance alone

- Low chi square values indicate a high probability that the observed deviations could be due to random chance alone
- High chi square values indicate a low probability that the observed deviations are due to random chance alone

- If the chi square value results in a probability that is less than 0.05 (ie: less than 5%) it is considered ***statistically significant***
  - The hypothesis is rejected

Standard Table for χ^2 and Fit Probability (P-value)

Degrees of Freedom	$P = 0.99$	0.95	0.80	0.50	0.20	0.05	0.01
1	0.000157	0.00393	0.0642	0.455	1.642	**3.841**	**6.635**
2	0.020	0.103	0.446	1.386	3.219	**5.991**	**9.210**
3	0.115	0.352	1.005	2.366	4.642	**7.815**	**11.345**
4	0.297	0.711	1.649	3.357	5.989	**9.488**	**13.277**
5	0.554	1.145	2.343	4.351	7.289	**11.070**	**15.086**
6	0.872	1.635	3.070	5.348	8.558	**12.592**	**16.812**
7	1.239	2.167	3.822	6.346	9.803	**14.067**	**18.475**
8	1.646	2.733	4.594	7.344	11.030	**15.507**	**20.090**
9	2.088	3.325	5.380	8.343	12.242	**16.919**	**21.666**
10	2.558	3.940	6.179	9.342	13.442	**18.307**	**23.209**

$P(\alpha, x) = \int_x^\infty t^{\alpha-1} e^{-t} dt$ where $x \equiv \chi^2/2$ and $\alpha \equiv dof/2$

Overestimation in CMS BH searches

CMS 2011 Data, 4.7 fb^{-1} [JHEP 04 (2012) 061]

S_T^{min}	N^{data}	N^{bkg}
Multiplicity $N \geq 3$		
2.4	667	690 ± 45
2.7	159	210 ± 28
2.8	95	140 ± 23
3.2	18	31 ± 11
Multiplicity $N \geq 4$		
2.5	245	280 ± 24
3.2	8	19 ± 6
3.6	1	4.6 ± 2.7
4.1	0	0.86 ± 0.9

CMS Results JHEP 04 (2012) 061

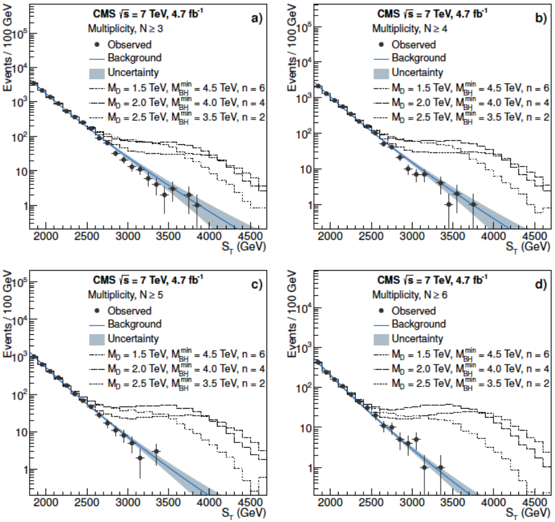

CMS Results JHEP 04 (2012) 061

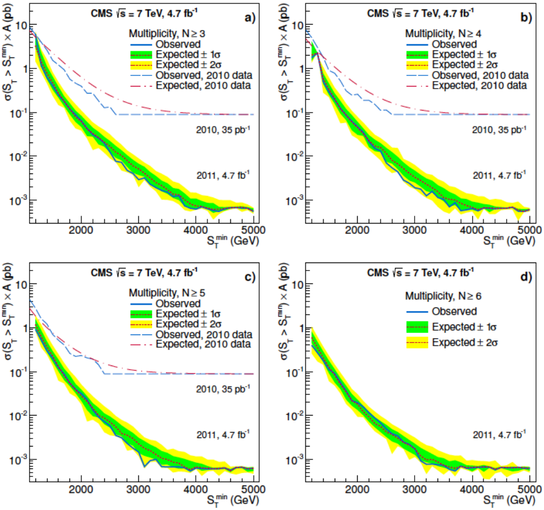

CMS Results JHEP 1307 (2013) 178